Research Article

IRS-Assisted Visible Light Communication for Improved Monitoring of Patient Vital Signals in Hospital Environment

Babak Sadeghi, and Seyed Mohammad Sajad Sadough[*] [iD]

Faculty of Electrical Engineering, Shahid Beheshti University, 1983969411 Tehran, Iran

* Corresponding Author:　s_sadough@sbu.ac.ir

Abstract: This paper explores the integration of intelligent reflecting surfaces (IRS) with visible light communication (VLC) to enhance optical communication reliability and mitigate link blockage. We particularly focus on a patient vital signal monitoring system in a hospital, where a wireless optical device-to-device (D2D) unit transmits signals to a monitoring center. Our study highlights the benefits of using an IRS, demonstrating that a 35-unit IRS array can double the received optical power compared to traditional non-line-of-sight (NLOS) links. We also propose an optimal placement strategy for IRS on indoor area walls to maximize the signal-to-noise ratio (SNR) and minimize the bit error rate (BER), considering constraints specific to optical wireless communication. We formulate and solve an optimization problem to determine the best IRS location, aimed at achieving ubiquitous communication with minimal BER. Numerical results illustrate the system's effectiveness in enhancing optical link reliability for patient monitoring. The findings indicate that optimal IRS placement can result in a BER as low as 2.48×10^{-8}, and with adjustments to the photodetector orientation, an even lower BER of around 6.32×10^{-10} can be achieved without increasing transmitter power. This research underscores the potential of IRS in improving the performance of VLC systems, particularly in critical applications such as healthcare monitoring.

Keywords: Intelligent reflecting surface (IRS), device-to-device (D2D), bit error rate (BER), non-line-of-sight (NLOS), vital signal monitoring system, signal to noise ratio (SNR).

How to cite this article
B. Sadeghi, and S. M. Sajad Sadough, "IRS-Assisted Visible Light Communication for Improved Monitoring of Patient Vital Signals in Hospital Environment," *J. Appl. Res. Electr. Eng*., Vol. 3, No. 2, pp. 241-249, 2024.
 DOI: 10.22055/jaree.2025.47734.1133

Check for
updates

1. INTRODUCTION

1.1. Background

Device-to-device (D2D) communication enables communication devices to be directly linked with each other without the need for a central base station [1]. For instance, efficient data sharing, collaboration between devices, and improved reliability in dense network environments can be achieved with D2D. In 6G, D2D communication can be further improved by utilizing visible light communication (VLC) [1]. D2D communication through VLC can enable local, fast, and efficient data transfer, by reducing the load on the overall network. Therefore, VLC can be a good option for machine-type communications (MTC) in the hospital

environment [1]. However, such a link can be blocked many times by people and objects especially in dense hospital environments. As depicted in Fig. 1, intelligent reflecting surface (IRS) helps us to overcome the blockage of direct or line-of-sight (LOS) links as well as the random orientation of receiver/transmitter in VLC links by modifying the configuration of the optical channel. In the lack of a LoS path, the IRS link can provide a connection with higher quality-of-service (QoS), more reliability and higher flexibility compared to the classical non-line of sight (NLOS) link (from a wall, sofa, etc.) in an indoor hospital environment [2]. By finding the optimal location of IRS units, the benefits of IRS can be increased and the probability of outage in LOS links can be reduced.
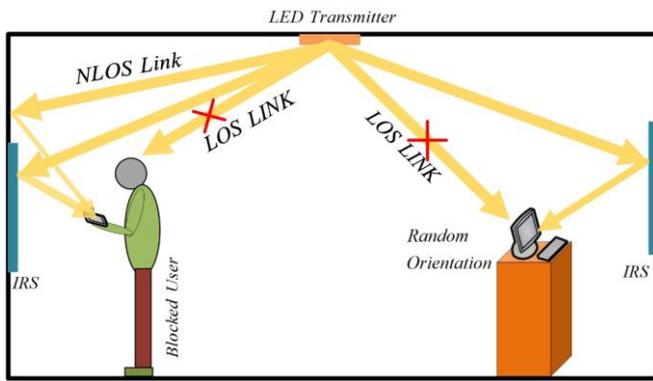
Fig. 1: Basic schematic of an IRS-assisted VLC system in overcoming the random orientation of the optical detector and link blockage.

Implementing intelligent reflecting surfaces (IRS) in a real-world hospital involves several technical issues such as [1-8]: **i)** site survey and assessment, to ensure optimal placement of IRS for effective coverage; **ii)** integration with existing infrastructure to avoid interference and ensure compatibility with existing wireless networks and medical devices; **iii)** accurate signal modeling is necessary due to the presence of walls, corridors, medical equipment, etc. that can attenuate the signal's strength; **iv)** staff training is crucial for successful deployment; **v)** signal quality index (SQI) should be considered as a metric to check the quality of the received signal, etc.

1.2. Related Works

Several studies have pointed out the pros and cons of combining IRS with indoor VLC communication (see for instance [4-10]).

The pioneering research in the field of using VLC as a transmission medium for monitoring the patient's vital signals was performed in [9, 10]. In these works, VLC is introduced as an emerging technology that can take over the role of radio frequency signals in hospital data transmission. These studies deal with general schematic of optical transmitters and receivers, but they do not mention the problems of applying visible light in transmitting and receiving data.

In [3], the authors have provided a depth literature survey of VLC-enabled patient monitoring systems and indoor localization where they present some of the major challenges and some of the open issues in the field of VLC-enabled healthcare.

In [4], the authors have compared meta-surface and mirror-type IRS where they have extracted the required phase changes of various reflecting surfaces for choosing an optimal power concentration method. However, in this study, the inherent constraints and required optimization of IRS are not addressed.

A framework for integrating IRS with indoor VLC systems is proposed in [5], where an overview of IRS and its advantages, different IRS types and its main applications in VLC systems are presented. Moreover, the authors have also investigated the capacity of IRS to overcome the effects of receiver's random orientation and blockage of optical links.

In [6], to tackle with receiver's random orientation, the authors have proposed an IRS-aided indoor VLC system with an optimal irradiance angle guided toward the user subject, which can facilitate optimal orientation of the IRS element in order to maximize the received power at the user's location. Moreover, the closed-form expression for the obtained optimal irradiance angle is derived. However, the optimal location of IRS units to guarantee a ubiquitous coverage is not addressed.

One of the few studies in the field of IRS parameter optimization, is done in [7] where the authors propose optimizing the IRS-assisted VLC systems by controlling the IRS elements to maximize the network sum-rate while maintaining fairness in the user achievable throughput.

One of the most relevant study in the field of patient vital signs monitoring is that presented in [8], where SQI is used to evaluate the quality of the optical link.

In most of these studies in the field of VLC, the use of IRS has been mentioned in order to improve the optical link performance, but almost none of them have addressed the challenges and constraints of its use. These challenges are divided into three main categories: challenges caused by the optical transmitter, optical receiver, and also the restrictions caused by the IRS.

1.3. Main Contributions

The main purpose of this paper is to address the advantages brought by IRS deployment and optimization of IRS placement for increasing the received SNR and BER in the indoor VLC system inside a hospital environment for the critical application of healthcare monitoring system. In brief, our main contributions can be summarized as follows.

- We prove the superiority of the IRS-assisted VLC link over the classic NLOS VLC link in the hospital indoor environment, by comparing the received power at the receiver's location.
- We derive the inherent constraints for deploying IRS in indoor visible light D2D communication.
- We formulate and numerically solve the optimization problem to determine the optimal location of IRS deployment leading to the minimum BER at the location of the optical receiver in the considered area.
- Although the main aim of this article is to find the optimal location of the IRS in order to increase the SNR and reduce the BER, in this article we also show that fine-tuning the orientation of the optical detector (PD) of the receiver, can be very effective for improving these parameters.

1.4. Paper Organization

The rest of this paper is structured as follows. In Section 2, we introduce the system model and the channel model of the IRS-assisted VLC healthcare monitoring system inside the considered hospital environment. In Section 3, we derive the limitations and the constraints regarding optimal placement of IRS inside the indoor area. These constraints are divided into three general categories of receiver constraints, transmitter constraints and IRS application restrictions. In Section 4, we consider the BER as the appropriate objective function that we minimize according to the constraints

derived in Section 3. In the rest of Section 4, we numerically solve the BER optimization problem to find the optimal placement of the IRS unit. Section 5 illustrates through simulations the superiority of the IRS-assisted VLC link over the classical NLOS link and also the advantages brought by optimizing the location of the IRS in terms of received SNR and BER. Finally, in Section 6, we draw our concluding remarks.

2. IRS-AIDED INDOOR VLC SYSTEM AND OPTICAL CHANNEL MODEL

Fig. 2 depicts the considered scenario of downlink VLC communication system. More precisely, we consider a non-coherent light-emitting diode (LED) access point (AP), oriented horizontally and installed on the platform of the room. The aim of the communication system is to measure vital signals of the patient located at height h_t in the hospital indoor environment of dimensions $L \times W \times H$. The receiver is a photodetector (PD) which is located at height h_r. In order to overcome blockage of the optical beam, an IRS array composed of N units is placed on the side wall, where angle diversity receiver (ADR) is also used. The location of AP and PD are assumed fixed, but their orientation can be changed. Fig. 3 implies the block diagram of the considered transmitter and receiver. As shown in Fig. 3, the intensity of the optical source is modulated with on-off keying (OOK) where the amplitude of symbols belongs to the set $\{0, A_{sym}\}$ and demodulation is performed by direct detection (IM/DD) of the optical beam and conversion to the photocurrent signal $y(t)$ by using a PD. We have:

$$y(t) = G_{oc} R x(t) \otimes h(t) + w(t) , \qquad (1)$$

where $x(t)$ is the radiated beam of the AP, generated from the modulated digital beam stream $S(t)$, G_{oc} is the gain of the optical

Fig. 2: Indoor hospital VLC system consisting of a transmitter and a receiver and an array of IRS.

Fig. 3: Block diagram of an IM/DD transceiver

concentrator, R is the responsivity of the optical detector, $h(t)$ is the baseband channel impulse response and $w(t)$ is the additive white Gaussian noise (AWGN) which is assumed independent from the data signal with probability density function $N(0, \sigma_T^2)$. Also, $h_m(t)$ is the matched filter impulse response, and $r(t)$ is the matched filter output, which is passed through the sampler working at nT_{sym} (T_{sym} is time of each symbol in OOK, $n \in \mathbb{N}$) to produce the discrete sequence r_n. According to (1) and the system model in Fig. 3, we have:

$$r(t) = [G_{oc} R x(t) \otimes h(t)] \otimes h_m(t) + w(t) \otimes h_m(t). \qquad (2)$$

By defining $v(t) = w(t) \otimes h_m(t)$, we get:

$$r(t) = [G_{oc} R x(t) \otimes h(t)] \otimes h_m(t) + v(t). \qquad (3)$$

The sampled symbol r_n at the output of the matched filter for the n-th bit can thus be expressed as follows:

$$r_n = \begin{cases} A_{sym} + v_n & ; \text{ if 1 is sent} \\ v_n & ; \text{ if 0 is sent} \end{cases}, \qquad (4)$$

where v_n is the sampled noise which is a Gaussian random variable.

In IRS-assisted indoor VLC, the channel gain is composed as the sum of three terms: i) the LOS channel component, ii) the NLOS channel components due to reflections from wall and objects, and iii) reflections from the IRS units. So, the total IRS-assisted VLC channel DC gain can be expressed as [11, 12]:

$$H = H_{los} \ P_{out} + \sum_{k=1}^{K} H_{nlos,k} + \sum_{n=1}^{N} H_{irs,n} , \qquad (5)$$

where H_{los} is the DC gain of the LOS channel, $H_{nlos,k}$ is the DC gain of the NLOS channel due to the k-th reflector ($k \in \{1, ..., K\}$) and $H_{irs,n}$ is the DC gain of the IRS channel due to the n-th unit ($n \in \{1, ..., N\}$). K and N are the number of reflectors in the room (wall, sofa, etc.) and the number of IRS elements, respectively. Moreover, in (2), we have assumed that the LOS link in the considered system model (hospital indoor environment) is blocked by humans (nurse, doctor, etc.) and/or objects, with a probability P_{out}.

2.1. LOS Channel Gain

The VLC channel DC gain corresponding the LOS component, is given as [2]:

$$H_{los} = \frac{A_{PD}(m_l + 1)}{2\pi d_{tr}^2} \cos^{m_l}(\phi) g(\psi) T(\psi) \cos(\psi) , \qquad (6)$$

where ϕ is the angle of irradiance, ψ is the angle of incidence, and $g(\psi)$ is a function of the refractive index and the semi-angle of the field-of-view ψ_{fov}; A_{PD}, m_l, $T(\psi)$, and d_{tr} denote the PD area, the Lambertian order, the optical filter gain, and the distance between the transmitter and the receiver, respectively [2].
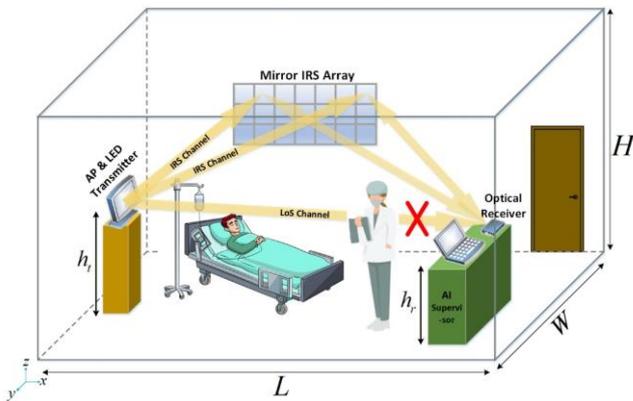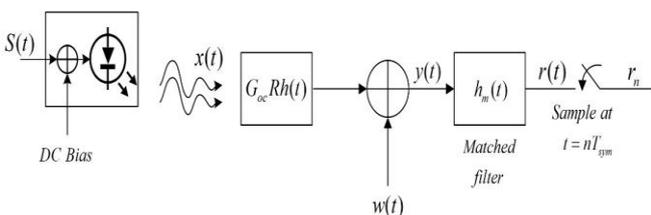
2.2. NLOS Channel Gain

In characterization of NLOS links, two general reflection model from the wall are commonly considered in the literature, namely the Lambertian model and the Phong model [4]. Here, to estimate the DC gain of the NLOS component, the Lambert's model is considered for reflection from the surfaces inside the room. The NLOS channel gain from the wall corresponding to the k -th reflector is defined as [2]:

$$H_{nlos,k} = \int_{A_{ref}} \frac{(m_l+1)}{2\pi d_{refr}^2 d_{tref}^2} \rho_{ref} \cos^{m_l}(\phi) T(\psi) g(\psi) \cos(\theta_i) \qquad (7)$$
$$\times \cos(\theta_r) \cos(\psi) \, dA_{ref} \, ,$$

where d_{tref} is the distance of the light source from the reflector, and d_{refr} is the distance between the reflector and the receiver. To increase the accuracy of NLOS channel DC gain estimation, we divide each reflector surface into small dA_{ref} surfaces with reflection coefficient ρ_{ref} ; θ_i and θ_r are the angles of incidence and reflection of the NLOS paths on the reflecting surfaces [13].

2.3. IRS Channel Gain

Let the effective area of each IRS unit be equal to ΔA_{irs} and the reflection coefficient for each unit ρ_i . The DC gain of the IRS channel with N serving units for one user, writes [14]:

$$H_{irs} = N \frac{A_{PD}(m_l+1)}{2\pi d_{ti}^2 d_{ir}^2} \rho_i \Delta A_{irs} \cos^{m_l}(\phi) T(\psi) g(\psi) \qquad (8)$$
$$\times \cos(\theta_{iirs}) \cos(\theta_{rirs}) \cos(\psi) \, ,$$

where d_{ti} is the distance between the light source and the n -th IRS unit and d_{ir} is the distance between the n -th IRS unit and the optical receiver, θ_{iirs} and θ_{rirs} are the angle of incidence with the IRS surface and the angle of reflection from the IRS surface, respectively [14].

3. PRACTICAL CONSTRAINTS REGARDING IRS DEPLOYMENT

In what follows, we address the important constraints that should be considered at the transmitter, IRS and receiver sides in order to reduce the probability of link outage to ensure a ubiquitous communication. As can be seen from Fig. 4, these constraints lead to restrictions on the location of IRS deployment. As shown in Fig. 4, we assume a 3D Cartesian coordinate system where IRS units are deployed across the x-axis, where y is fixed (x and z are variable). The limitations caused by AP will determine the lower limit on the x-axis, denoted by x_l, and the limitations caused by the photoreceptor and IRS can determine the upper limit of the use of IRS on the x-axis, that we denote by x_h.
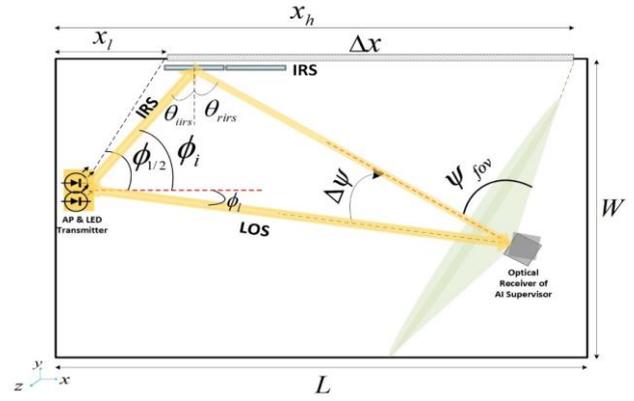
Fig. 4: Constraints affecting the placement of IRS in VLC communication (top view of the hospital room).

3.1. Constraints Related to the Optical Transmitter

The first constraint is related to the optical transmitter i.e., the visible light source. Usually, in VLC systems, the Lambertian order (denoted m_l) of the source, which characterizes the directivity of the radiation beam, is one of the effective factors in determining the half-power angle ($\phi_{1/2}$), i.e., the illumination and communication coverage radius of the source [2].

As seen from Fig. 5, the increase of m_l causes the decrease of $\phi_{1/2}$. The decrease in $\phi_{1/2}$, in turn, narrows the width of the beam which causes the light beam to reach the walls at a larger vertical distance from the light source, which itself creates a lower limit for the placement of the IRS on the x-axis (see Fig. 4). Mathematically, for a light source of Lambertian order m_l , $\phi_{1/2}$ is expressed as [2]:

$$\phi_{1/2} = cos^{-1}(exp(-\frac{ln2}{m_l})) \, . \qquad (9)$$

If an optical AP of Lambertian order m_l is located at the coordinate (x_T, y_T, z_T), the first point on the wall that is within the teleradius of the source will be located at a longitudinal distance x_l from the origin [15].
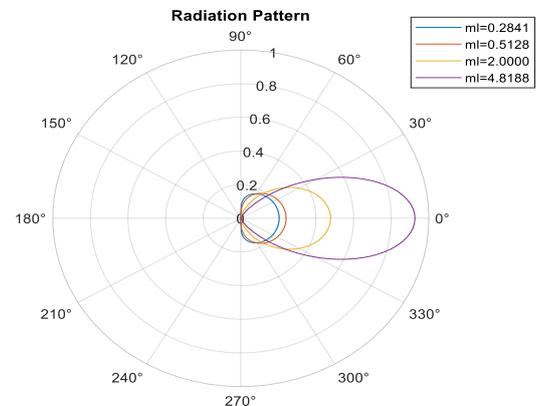
Fig. 1: Radiation pattern of the transmitter with different Lambertian order.

More precisely, x_l is the lower limit allowed for the deployment of IRS, which is expressed as [13]:

$$x_l = x_T + \frac{\left|-w - y_T\right|}{\tan(\phi_{1/2})}. \tag{10}$$

It is worth mentioning that another important limiting factor related to the AP is its transmission power, which is usually limited by the sensitivity of human eyes and skin as well as hardware limitations of the transmitter [16].

3.2. Constraints Related to the IRS

Since the function of mirror IRS is based on the formation of a virtual image (see Fig. 6), as a result, the IRS units must receive a light beam with an angle of incidence of less than 90 degrees from the light source. So, a limit should be considered for the allowed rotation of the IRS elements or equivalently the phase shift of the reflection beam, according to its location [17].

Let us assume that an IRS is located at coordinate (x_I, y_I, z_I), then the maximum angle that the IRS can rotate around x and z axes can be expressed as [17]:

$$
\begin{aligned}
\theta_{\max} = \phi_{rotl} &= \tan^{-1}\left(\frac{\sqrt{(z_I - z_T)^2 + (y_I - y_T)^2}}{(x_I - x_T)}\right) \\
&= \tan^{-1}\left(\frac{\sqrt{(z_I - h_t)^2 + (-w - y_T)^2}}{(x_I - x_T)}\right).
\end{aligned} \tag{11}
$$

By reducing $(x_I - x_T)$, i.e., the longitudinal distance between IRS and AP, IRS units are able to cover a wider area. Notice that since the minimum value of x_I is equal to x_l, this value is lower bounded by $(x_l - x_T)$.
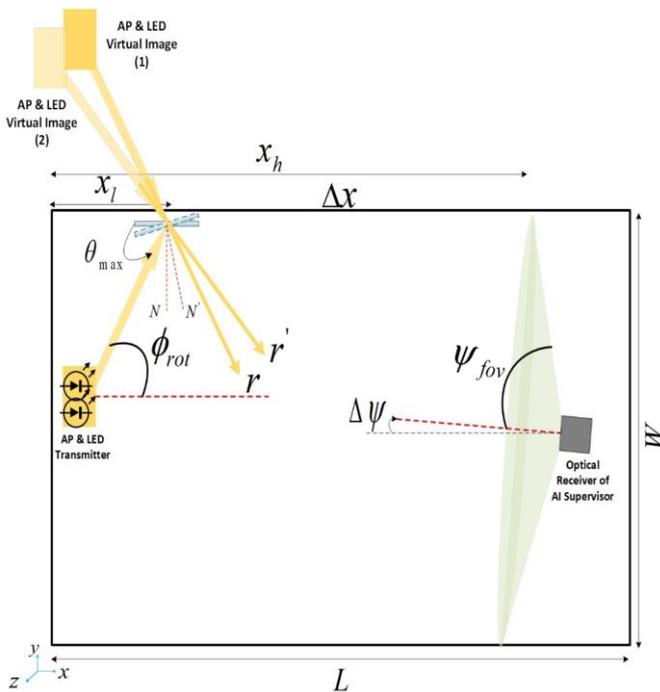
3.3. Constraints Related to the PD

The field of view (FOV) of the optical detector (as well as its orientation) is the third limiting factor in deploying IRS in a VLC system. As can be seen from Fig. 7, according to the FOV of the detector and its orientation, the deployment location of the IRS is limited. As depicted in Fig. 7, by a counter-clockwise orientation, the length of the allowed IRS installation area on the wall is reduced by Δx_d, and in contrast, with a clockwise orientation, the length of the IRS installation area on the wall is increased by Δx_i. In practice, by adjusting the PD orientation, the SNR and as a result the length of the allowable area can be increased, but since in the usual case, the LOS link is responsible for the communication between the optical transmitter and the receiver, we will have a compromise in the PD orientation setting. So, in a way, the upper limit of the length of the allowed area for using IRS, i.e., x_h, and even the selection of the proper side wall for the purpose of engaging IRS is determined according to the orientation of PD.

In calculating the upper limit x_h, the deployment location of PD and its orientation play a role. Assuming that the location of the receiver is (x_r, y_r, z_r) and its initial random orientation is $\pm \Delta \psi$, we have:

$$x_h = x_{ori} = x_r - \frac{\left|-w - y_r\right|}{\tan(\psi_{fov} \pm \Delta \psi)}, \tag{12}$$

where x_{ori} is the limitation due to the orientation of the PD, ψ_{fov} is the FOV of the optical detector and $\Delta \psi$ is considered positive in PD clockwise rotation and negative in counterclockwise rotation.

4. OPTIMIZATION OF IRS LOCATION

In this Section, we propose to optimize the place of IRS inside the considered room so as to minimize the BER at the receiver by considering the constraints we discussed in

Fig. 6: Coverage profile of the optical transmitter, taking into account the geometry of the image formation and the constraints caused by it.
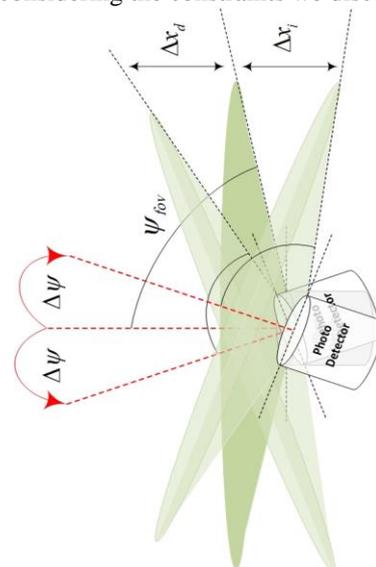
Fig. 7: Effect of FOV and PD orientation in determining the allowable area of IRS deployment.

Section 3. According to the system model in Section 2, the probability of error at the receiver for OOK modulation, is expressed as [2]:

$$P(error) = P(0)P(error|0) + P(A_{sym})P(error|A_{sym}). \tag{13}$$

By assuming probability of each symbol $P(A_{sym}) = P(0) = P(1) = 0.5$, we get:

$$P(error) = \frac{1}{2}Q(\frac{A_{sym}}{\sigma_T}) + \frac{1}{2}Q(\frac{A_{sym}}{\sigma_T}) = Q(\frac{A_{sym}}{\sigma_T}) = Q(\sqrt{\gamma}), \tag{14}$$

where $\gamma = SNR = \frac{A_{sym}^2}{\sigma_T^2}$ and $Q(x) = \frac{1}{\sqrt{2\pi}}\int_x^\infty e^{-\lambda^2/2}d\lambda$.

Let us define $i_{ph} = i_{ph_{los}} + i_{ph_{nlos}} + i_{ph_{irs}}$ as the photocurrent caused by the received optical signal, which is the sum of three components: $i_{ph_{los}}, i_{ph_{nlos}}, i_{ph_{irs}}$ are the photocurrent caused by the LOS, NLOS and IRS links, respectively. We assume that the noise variance $\sigma_T^2 = \sigma_{sh}^2 + \sigma_{th}^2$ where σ_{sh}^2 and σ_{th}^2 are the shot noise variance and the thermal noise variance, respectively, that are assumed as the dominant noises in our scenario. The probability of error in Eq. (14) can be equivalently expressed as [2]:

$$P_{e_{ook}} = Q(\sqrt{\gamma}) = Q(\frac{G_{oc}RP_r}{\sigma_T}) = Q(\frac{i_{ph}}{\sigma_T}). \tag{15}$$

Since $y(t)$ in the system model is the photocurrent created in PD due to the received Power P_r, so its signal part i_{ph} corresponds to the transmitted symbol A_{sym} [2, 13], hence we will have:

$$P_{e_{ook}} = Q(\sqrt{\gamma}) = Q(\frac{i_{ph}}{\sigma_T}) = Q(\frac{i_{ph_{los}} + i_{ph_{nlos}} + i_{ph_{irs}}}{\sqrt{\sigma_{sh}^2 + \sigma_{th}^2}}). \tag{16}$$

Assuming that the impact of the NLOS link is negligible, $i_{ph_{nlos}}$ can be omitted. According to [2], the shot noise can be written as $2q(i_{ph_{los}} + i_{ph_{irs}})B_{sys}$ and the thermal noise as $4k_bTB_{sys}R_l^{-1}$, where q is the electric charge, B_{sys} is the bandwidth of the optical receiver, R_l is the load resistance, T is the absolute temperature, and k_b is the Boltzmann's constant. Eq. (16) can thus be rewritten in an equivalent form as:

$$P_{e_{OOK}} = Q(\frac{i_{ph_{los}} + i_{ph_{irs}}}{\sqrt{2q(i_{ph_{los}} + i_{ph_{irs}})B_{sys} + 4k_bTB_{sys}R_l^{-1}}}). \tag{17}$$

Considering that the photocurrent is a function of the received power, since, the received power is a function of the transmitted power P_t [2], Eq. (17) can be written as follows:

$$P_{e_{ook}} = Q(\frac{G_{oc}RH_{los_i}P_t + G_{oc}RH_{irs_i}P_t}{\sqrt{2q(G_{oc}RH_{los}P_t + G_{oc}RH_{irs_i}P)B_{sys} + 4k_bTB_{sys}R_l^{-1}}}). \tag{18}$$

As can be seen from (18), the photocurrent due to the NLOS link has been neglected. The numerical comparison results of IRS-based and NLOS-based VLC links are contrasted in the next section.

Now, to calculate the optimal location of the IRS, we formulate the following optimization problem:

$$\{\hat{x}_I, \hat{z}_I\} = \underset{x_l \leq x_I \leq x_h, \ 0 \leq z_I \leq H}{\arg\min} BER, \tag{19}$$

which can be expressed by using (18) as:

$$\{\hat{x}_I, \hat{z}_I\} = \underset{x_l \leq x_I \leq x_h, \ 0 \leq z_I \leq H}{\arg\min} Q(\frac{G_{oc}RH_{los}P_t + G_{oc}RH_{irs}P_t}{\sqrt{2q(G_{oc}RH_{los}P_t + G_{oc}RH_{irs}P_t)B_{sys} + 4k_bTB_{sys}R_l^{-1}}}). \tag{20}$$

According to the basic properties of the Q-function, (20) can be rewritten in an equivalent form as:

$$\{\hat{x}_I, \hat{z}_I\} = \underset{x_l \leq x_I \leq x_h, \ 0 \leq z_I \leq H}{\arg\max} \left[\frac{G_{oc}RH_{los}P_t + G_{oc}RH_{irs}P_t}{\sqrt{2q(G_{oc}RH_{los}P_t + G_{oc}RH_{irs}P_t)B_{sys} + 4k_bTB_{sys}R_l^{-1}}}\right]. \tag{21}$$

Finally, assuming that the LOS link is blocked ($H_{los} \simeq 0$) and the NLOS link is also not reliable due to the inability to control the reflection beam and choose the reflection model, we get:

$$\{\hat{x}_I, \hat{z}_I\} = \underset{x_l \leq x_I \leq x_h, \ 0 \leq z_I \leq H}{\arg\max} \left[\frac{G_{oc}RH_{irs}P_t}{\sqrt{2qG_{oc}RH_{irs}P_tB_{sys} + 4k_bTB_{sys}R_l^{-1}}}\right]. \tag{22}$$

Considering shot noise limited condition [2] (i.e., all other noises can be neglected except the shot noise), Eq. (22) can be written in an equivalent form as:

$$\{\hat{x}_I, \hat{z}_I\} = \underset{x_l \leq x_I \leq x_h, \ 0 \leq z_I \leq H}{\arg\max} \left[\frac{H_{irs}}{\sqrt{2qH_{irs}B_{sys}}}\right]. \tag{23}$$

In fact, the optimization problem (19) becomes equivalent to finding $\hat{x}_I$ and $\hat{z}_I$ by maximizing H_{irs}, because the noise parameters q and B_{sys} are almost constant values and the Eq. (23) is simplified to $\frac{H_{irs}}{\sqrt{H_{irs}}}$. So we can write:

$$\{\hat{x}_I, \hat{z}_I\} = \underset{x_l \leq x_I \leq x_h, \ 0 \leq z_I \leq H}{\arg\max} H_{irs}. \tag{24}$$

In (24), H_{irs} is a function of distances and angles (see Eq. (8)), which in turn are functions of x_I and z_I. Therefore, H_{irs} will also be a function of x_I and z_I. If $\hat{x}_I$ and $\hat{z}_I$ maximize H_{irs}, then the following condition must hold:

$$H_{irs}(x_I, z_I) \leq H_{irs}(\hat{x}_I, \hat{z}_I), \tag{25}$$

where $x_l \leq x_I \leq x_h$, $0 \leq z_I \leq H$. For (25) to be satisfied, the directional derivative of H_{irs}, with respect to x and z, must be zero at $\hat{x}_I$ and $\hat{z}_I$. That is why we can write:

$$\left(H_{irs x_I}(\hat{x}_I, \hat{z}_I), H_{irs z_I}(\hat{x}_I, \hat{z}_I)\right) = (0, 0). \tag{26}$$

where $H_{irs x_I}(\hat{x}_I, \hat{z}_I)$, $H_{irs z_I}(\hat{x}_I, \hat{z}_I)$ are the derivatives of H_{irs} with respect to x_I and z_I respectively. The values of x_I and z_I that maximize H_{irs} characterize the optimal location of IRS leading to minimization of the average BER at receiver that are obtained in the next section through numerical optimization.

5. NUMERICAL OPTIMIZATION AND SIMULATION RESULTS

Here, we propose to evaluate the performance of the considered IRS-assisted VLC system by particularly focusing on the effect of IRS placement. The simulation environment is graphically depicted in Fig. 2. The main values and assumptions considered throughout simulations are provided in Table 1.

In Table 2, we have gathered the limit of parameters related to IRS deployment on the side wall (by assuming $y_I = -5$), according to the constraints described in Section 3.

By evaluating the BER at different places of the allowed region, we place the IRS unit at coordinate where BER is minimal.

We focus on received power and BER at the receiver location achieved by using IRS in VLC link compared to classical NLOS, under practical constraints described in Section 3.

Table 1: Parameters and assumptions

Parameter	Value	Description
$L \times W \times H$	5m×5m×3m	Room dimensions (Length, width, height) (m)
(x_T, y_T, z_T)	$(0.5, -3.5, 1.5)$	Coordinates of the transmitter's location (m)
(x_r, y_r, z_r)	$(4, -1, 1.5)$	Coordinates of the receiver's location (m)
m_l	0.4	Lambertian order of optical transmitter
ψ_{fov}	80	Field of view of the PD (degree)
$\phi_{1/2}$	80	Half power angle (degree)
$\Delta\psi$	5	PD orientation (degree)
A	0.0004	Effective area of the PD (m^2)
R	1	PD Responsivity
$T(\psi)$	١	Optical filter gain
N	35	Number of IRS units
$a \times a$	0.1m×0.1m	Dimensions of IRS units (m^2)
n_i	1.5	Concentrator internal refractive index
R_b	1 Gbps	Data rate (bps)
ρ_{ref}	0.5	Reflection coefficient of wall
ρ_i	0.9	Reflection coefficient of IRS units
P_t	200	Transmitted Power (Watts)

Table 2: Calculated constraints regarding IRS installation

Parameter	Description	Value/unit
x_l	Lower limit length of the allowed region for deployment of the IRS.	1.1145 m
x_h	Upper limit length of the allowed region for deployment of the IRS.	3.3 m
θ_{max}	Allowed rotation range of IRS units at the optimal deployment point (degree).	$[30, 65]$ degree

Fig. 8 depicts the received power when using the classical NLOS VLC link by considering the reflections from wall surface at different locations of the allowed region according to the Phong reflection model [18]. We can observe that as the reflector approaches the coordinate $(x_l, -W, z_T)$, the received power is increased up to about 5.85×10^{-9} watts. If we consider the entire allowed region can be dedicated as reflector, the received power is even increased up to 5.1245×10^{-4} watts.

Fig. 9 shows the received power at different locations of the considered area when a 35 unit array IRS is used (all 35 units serve the PD) at that location. We observe that, as the IRS approaches the location $(x_l, -W, z_T)$ which is the optimal point of IRS deployment, the received power increases (up to about 11×10^{-4} watts). By comparing Figs. 8 and 9, we can see that the power received in the IRS link increases more than twice, i.e., about $3\,dB$, compared to the classic NLOS link which proves the significant advantage of employing IRS in our system model (the entire allowed area of the reflector surface is taken into account).

Fig. 10 illustrates the BER comparison (plotted based on the theoretical BER of Eqs. (15) and (18)) at the receiver in
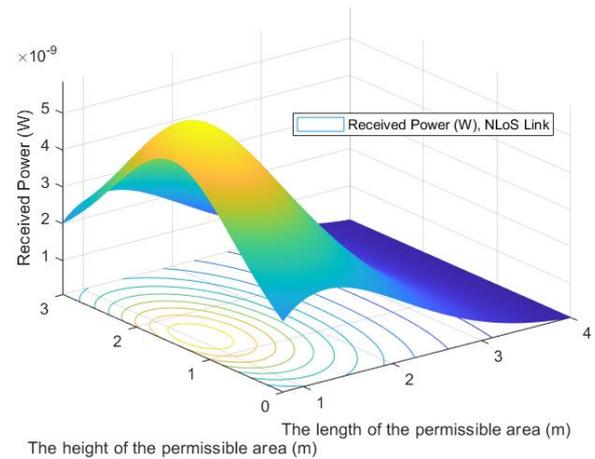
Fig. 8: The received power of the optical receiver considering the entire allowed area as reflective surface in the classical NLOS VLC link.
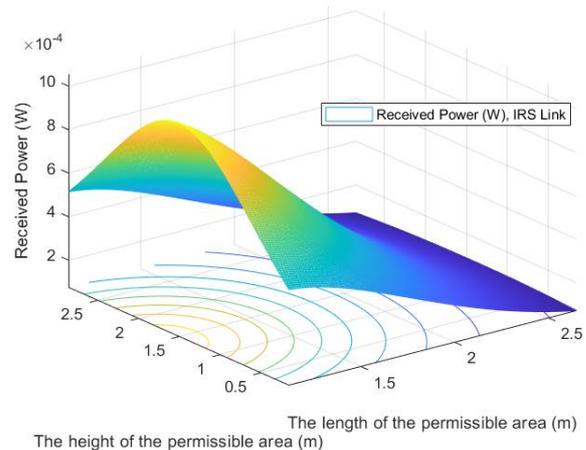
Fig. 9: The received power of the optical receiver at different locations of the considered area by using a 35 unit IRS.

NLOS and IRS links. More precisely, in Fig. 10, by changing the transmitter power in the range $16 < P_t < 29\ dB$, we get $-8 < SNR < 4.7\ dB$ at the receiver through NLOS link and $-4.7 < SNR < 8\ dB$ at the IRS-aided VLC link. These results confirm the superiority and also the reliability (in terms of QoS and SNR) [19] of IRS-aided VLC link compared to classic NLOS link in terms of BER.

Fig. 11 shows the BER variations versus location of the IRS for three different locations of the optical receiver. Notice that according to our system model, in the indoor hospital environment, the IRS cannot be placed across the y axis. So for each location of the receiver, the minimum of each curve is the optimal location of the IRS for its deployment in the allowed area. Considering these three curves, it can be concluded that the minimum BER values always occurs regardless of the location of the receiver when the IRS is located at the $(x_I, -W, z_T)$ coordinate, which is the optimal installation point.

Fig. 12 shows the BER variations for different PD orientations $\{-10°, 0, +10°\}$. We can particularly observe that when the transmit power changes in the range

$16 < P_t < 29\ dB$, the BER can be reduced to a desired value by fine-tuning the PD orientation.

Finally, Fig. 13 plots the received SNR versus the Lambertian order of the source (m_l) in different lengths of the allowed area ($z_I = 1.5\ m\ \&\ y_I = -5\ m$). As can be seen, by increasing m_l, the length of the lower bound of the allowed area i.e., x_l which is the coordinate of the optimal place of IRS deployment, is increased (the length of the upper limit of the allowed area x_h is assumed fixed).
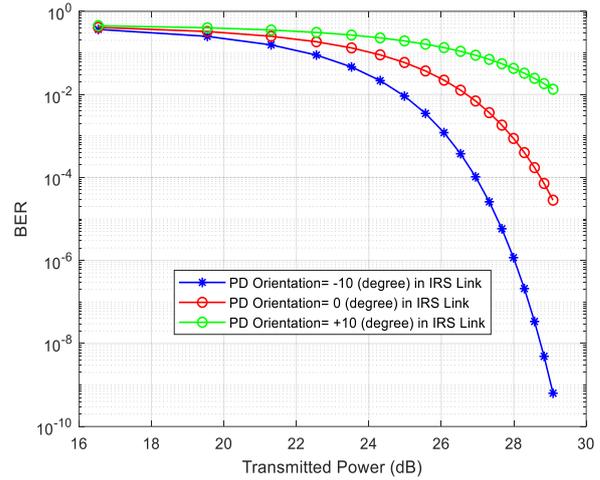
Fig. 3: The BER obtained in the receiver, caused by changes in the power of the optical transmitter as well as the different orientation of the PD, assuming that the noise power is constant.
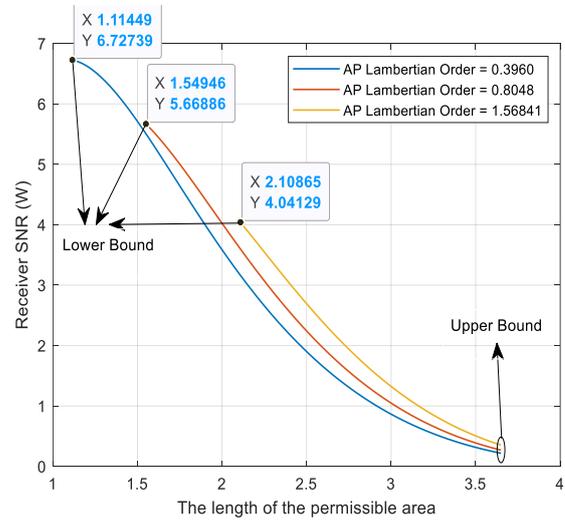
Fig. 13: Demonstration of the receiver SNR according to the location of the IRS in the allowed area, considering APs with three different Lambertian orders.

6. CONCLUSIONS

Optimal placement of IRS on the wall in order to minimize the BER at the receiver for an indoor VLC system was addressed. In this study, an optical AP and a photo-detector have been used to send and monitor the vital signals of a patient in a hospital environment. For the case where the LOS path is blocked in the VLC link, both the IRS directed link and the classical NLOS link have been considered. Comparative numerical results proved the superiority of the IRS-aided VLC link in terms of BER. Moreover, the power

Fig. 10: Comparison of BER in IRS-based optical link and classic NLOS-based optical link according to the transmitted power.

Fig. 2: BER curve resulting from variations in optical IRS location across the allowed region, considering three different locations for the optical receiver.

received through the IRS link is increased up to 2 times. Then, in order to have a reliable and ubiquitous connection, with the aim of minimizing the BER, the location of IRS installation was optimized. We also showed that by fine-tuning the PD orientation, even lower BER can be obtained. Finally, we showed that by increasing the Lambertian order, the optimal location of IRS deployment is shifted away from the source. The use of more complex optimization methods with multiple sources, multiple IRS arrays and fine tuning PD orientation can be considered as attractive future research directions in this field.

CREDIT AUTHORSHIP CONTRIBUTION STATEMENT

Babak Sadeghi: Conceptualization, Formal analysis, Investigation, Software, Roles/Writing - original draft. **Seyed Mohammad Sajad Sadough**: Project administration, Supervision, Writing - review & editing.

DECLARATION OF COMPETING INTEREST

The authors declare that they have no known competing financial interests or personal relationships that could have appeared to influence the work reported in this paper. The ethical issues; including plagiarism, informed consent, misconduct, data fabrication and/or falsification, double publication and/or submission, redundancy has been completely observed by the authors.

REFERENCES

[1] Hetvi Shah, Ajay K. Vyas, "A systematic review for 6G and beyond 6G enable IoT Network," IEEE 2024 2nd International Conference on Computer, *Communication and Control*, 2024.

[2] Z Ghassemlooy, W Popoola, S Rajbhandari, "Optical Wireless Communications: System and Channel Modelling with MATLAB®," *Taylor &Francis*, 2012.

[3] Harrison Kurunathan, R. Indhumathi, Miguel Gutiérrez Gaitán, Carla Taramasco, Eduardo Tovar, "VLC-enabled monitoring in a healthcare setting: Overview and Challenges," *IEEE Conference on Visible Light Communications*, December 2023.

[4] Amr M. Abdelhady, Ahmed K. Sultan, Osama Amin, Basem Shihada, and Mohamed-Slim Alouini, "Visible Light Communications via Intelligent Reflecting Surfaces: Metasurfaces vs Mirror arrays," *IEEE Open Journal of the Communications Society (Volume: 2)*, December 2020.

[5] Mohamed Amine Arfaoui, Ali Ghrayeb, and Chadi Assi, "Integration of IRS in Indoor VLC Systems: Challenges, Potential and Promising Solutions," *arXiv: 2101.05927 [eess.SP]*, January 2020.

[6] Mohit Bhar, Sameer Kumar, Anand Singh, "On the Optimal Evaluation of the Angle of Irradiance and the Orientation for an IRS-aided Indoor VLC," *TechRxiv*. May 11, 2023.

[7] Salah Abdeljabar, Mahmoud Wafik Eltokhey, Mohamed Slim Alouini, "Sum Rate and Fairness Optimization in RIS-Assisted VLC Systems," *IEEE Open Journal on the Communications Society*, April 2024.

[8] Amel Chehbani, Stephanie Sahuguede, Anne Julien-Vergonjanne, OlivierBernard, "Quality Indexes of the ECG Signal Transmitted Using Optical Wireless Link," *Sensors*, May 2023.

[9] K.Mahalakshmi, M.Sivaram, K. Shantha Kumari, D.Yuvaraj, R.Keerthika, "Healthcare Visible Light Communication," *International Journal of Pure and Applied Mathematics*, 2018.

[10] Abdulla Al-Qahtani, Hamad Al-hajri, Saad Al-kuwari, Naseer Al-yaarabi, Abdulrahman Al-hababi, Essa Al-kubaisi, Abdulla Ahmed, Mohamad Kashef and Qammer H. Abbasi, "An non-invasive remote health monitoring system using visible light communication," *International Journal of Pure and Applied Mathematics*, 2018.

[11] Özgecan Özdogan, Emil Björnson, E. Larsson , "Intelligent Reflecting Surfaces: Physics, Propagation, and Pathloss Modelling," *IEEE Wireless Communications Letters*, 2019.

[12] Milton Román Cañizares, Pablo Palacios Játiva, Javier Guaña-Moya, William Villegas-Ch and Cesar Azurdia-Meza, "On the Performance of Intelligent Reconfigurable Surfaces for 6G Indoor Visible Light Communications Systems," *Photonics*, 2023.

[13] Harald Haas, Mohammad Sufyan Islim, Cheng Chen, Hanaa Abumarshoud, "An Introduction to Optical Wireless Mobile Communication," *Artech House*, September 2021.

[14] Shiyuan Sun, Tengjiao Wang, "Intelligent Reflecting Surface-Aided Visible Light Communications: Potentials and Challenges," *IEEE Vehicular Technology Magazine*, 2021.

[15] Mahmoud Mohammadi, Seyed Mohammad Sajad Sadough, "Improved LED arrangement through outage probability minimization in LiFi communication systems," *The Institution of Engineering and Technology*, February 2023.

[16] Anand Singh, Haythem Bany Salameh, Moussa Ayyash, Hany Elgala, "Performance Analysis of OIRS-Aided Indoor VLC Systems under Dynamic Human Blockages and Random UE Orientation," *TechRxiv*. October 18, 2023.

[17] Qi Wu, Jian Zhang and Jia-Ning Guo, "Position Design for Reconfigurable Intelligent-Surface-Aided Indoor Visible Light Communication Systems," *Electronics*, 2022.

[18] Jan Burke, Alexey Pak, Sebastian Höfer, Mathias Ziebarth, Masoud Roschani, Jürgen Beyerer, "Deflectometry for specular surfaces: an overview," *Advanced Optical Technologies*, July 2023.

[19] Yufeng Zheng, Peng He, Yaping Cui, Ruyan Wang, Dapeng Wu, "Reliability optimization in IRS-assisted UAV networks," *Vehicular Communications*, May 2023.